https://doi.org/10.1093/plphys/kiac311 PLANT PHYSIOLOGY 2022: 190: 1321–1333

Plant Physiology®

Research Article

A calmodulin-like protein (CML10) interacts with cytosolic enzymes GSTU8 and FBA6 to regulate cold tolerance

Shuhan Yu,[1] Jiaxuan Wu,[1] Yanmei Sun,[1] Haifeng Zhu ,[1] Qiguo Sun,[1] Pengcheng Zhao ,[1] Risheng Huang[1] and Zhenfei Guo [1,*]

1 College of Grassland Science, Nanjing Agricultural University, Nanjing 210095, China

*Author for correspondence: zfguo@njau.edu.cn

S.Y., J.W., and Y.S. performed the experiments. S.Y., H.Z., Q.S., R.H., and P.Z. analyzed the experimental results. S.Y. and Z.G. wrote the manuscript. Z.G. conceived the research and designed the experiments.

The author responsible for distribution of materials integral to the findings presented in this article in accordance with the policy described in the Instructions for Authors (https://academic.oup.com/plphys/pages/general-instructions) is Zhenfei Guo (zfguo@njau.edu.cn).

Abstract

Calmodulin-like proteins (CMLs) are calcium (Ca^{2+}) sensors involved in plant growth and development as well as adaptation to environmental stresses; however, their roles in plant responses to cold are not well understood. To reveal the role of MsCML10 from alfalfa (*Medicago sativa*) in regulating cold tolerance, we examined transgenic alfalfa and *Medicago truncatula* overexpressing *MsCML10*, *MsCML10*-RNAi alfalfa, and a *M. truncatula cml10-1* mutant and identified MsCML10-interacting proteins. *MsCML10* and *MtCML10* transcripts were induced by cold treatment. Upregulation or downregulation of *MsCML10* resulted in increased or decreased cold tolerance, respectively, while *cml10-1* showed decreased cold tolerance that was complemented by expressing *MsCML10*, suggesting that MsCML10 regulates cold tolerance. MsCML10 interacted with glutathione S-transferase (MsGSTU8) and fructose 1,6-biphosphate aldolase (MsFBA6), and the interaction depended on the presence of Ca^{2+}. The altered activities of Glutathione S-transferase and FBA and levels of ROS and sugars were associated with *MsCML10* transcript levels. We propose that MsCML10 decodes the cold-induced Ca^{2+} signal and regulates cold tolerance through activating MsGSTU8 and MsFBA6, leading to improved maintenance of ROS homeostasis and increased accumulation of sugars for osmoregulation, respectively.

Introduction

Cold stress adversely affects crop growth, productivity, and quality. Temperate plants increase their survival during freezing temperatures through a cold acclimation (CA) mechanism. Thousands of genes are reprogrammed in expression during CA, some of which encode key enzymes involved in antioxidant defense and biosynthesis of osmolytes such as soluble sugars and proline (Zhu, 2016). The antioxidant defense system functions to scavenge reactive oxygen species (ROS) which is usually accumulated under low-temperature conditions as a result of inhibition of Calvin–Benson cycle enzymes that limit the use of absorbed light energy by CO_2 assimilation to maintain cell redox homeostasis (Suzuki et al., 2012). The antioxidant system consists of antioxidant enzymes, such as superoxide dismutase, catalase, ascorbate peroxidase, and glutathione (GSH) reductase, and nonenzyme antioxidants such as ascorbate, reduced GSH.

Received January 24, 2022. Accepted June 04, 2022. Advance access publication June 25, 2022

Glutathione S-transferase (GST) is also an antioxidant enzyme that regulates multiple abiotic stress tolerance using GSH as a substrate to scavenge ROS (Xu et al., 2016).

Free calcium (Ca^{2+}) is a universal signal involved in multiple cellular responses in plants (Reddy et al., 2011). Low temperature triggers Ca^{2+} channel activation, leading to a transient rise of free Ca^{2+} in the cytosol (Ding et al., 2019). The Ca^{2+} signal is perceived by Ca^{2+}-binding proteins or Ca^{2+} sensors containing one to four helix–loop–helix structures called EF-hand motif(s) (Reddy et al., 2011). There are four types of Ca^{2+} sensors in plants, including calmodulin (CaM), CaM-like protein (CML), calcineurin B-like protein (CBL), and Ca^{2+}-dependent protein kinase (CPK/CDPK) to decode Ca^{2+} signal by activating downstream proteins. CMLs in plants are specifically involved in the regulation of plant growth and development as well as responses to abiotic and biotic stresses (Reddy et al., 2011). Fifty *CMLs* have been identified in the genomes of Arabidopsis (*Arabidopsis thaliana*) and *Medicago truncatula* (Sun et al., 2020). In Arabidopsis, CML8, CML9, CML11, CML24, CML41, and CML43 are involved in plant innate immunity against bacteria (Chiasson et al., 2005; Ma et al., 2008; Leba et al., 2012; Cheng et al., 2016; Xu et al., 2017; Zhu et al., 2017), while CML9, CML20, CML37, and CML42 are responsive to abiotic stresses and regulate drought and salt tolerance positively or negatively (Magnan et al., 2008; Vadassery et al., 2012; Scholz et al., 2015; Wu et al., 2017; Zhu et al., 2022). CML24, CML25, CML36, and CML39 are involved in the regulation of flowering, pollen germination, and pollen tube elongation, or seed development and germination (Yang et al., 2014; Wang et al., 2015; Astegno et al., 2017; Midhat et al., 2018). In addition, CML10 interacts with phosphomannomutase and modulates stress responses by regulating ascorbate biosynthesis (Cho et al., 2016). CML24 regulates actin cytoskeleton and circadian oscillations through activating the circadian oscillator gene *TIMING OF CAB2 EXPRESSION1* (Ruiz et al., 2018), and it regulates ALUMINUM-ACTIVATED MALATE TRANSPORTER1-dependent Al tolerance through interacting with CALMODULIN BINDING TRANSCRIPTION ACTIVATOR2, and WRKY46 (Zhu et al., 2022). CML38 confers inhibition of root growth through interacting with rapid alkalinization factor 1 (Campos et al., 2018). Overexpression of *ShCML44* from wild tomato (*Solanum habrochaites*) results in enhanced multiple tolerance to cold, drought, and salinity stresses in transgenic tomato (*Solanum lycopersicum*; Munir et al., 2016). *CsCML16*, *CsCML18-2*, *CsCML38*, and *CsCML42* are responsive to low temperature, salinity, and drought in tea plants (*Camellia sinensis*; Ma et al., 2019).

Alfalfa (*Medicago sativa*) is the most important perennial forage legume due to its excellent nutritional quality and high productivity. The difference in cold tolerance among alfalfa cultivars is associated with the accumulated sugars or total nonstructure carbohydrate levels in roots during CA (Cunningham et al., 2001; Seppanen et al., 2018). Higher levels of cryoprotective compounds such as raffinose family oligosaccharides (RFOs), sucrose, and proline are accumulated in the recurrently selected populations with superior freezing tolerance compared with the initial backgrounds during CA (Castonguay et al., 2011). Similarly, higher levels of soluble sugars such as sucrose, *myo*-inositol, galactinol, and raffinose are observed in *M. sativa* subsp. *Medicago falcata* (L.), which is closely related to alfalfa, with greater cold tolerance than in alfalfa or in *M. truncatula*, a leguminous model plant with low cold tolerance, during CA (Zhang et al., 2011; Tan et al., 2013; Zhuo et al., 2013). In addition, the regulation of several cold-responsive genes from *M. falcata*, such as *S-ADENOSYLMETHIONINE SYNTHETASE*, *ETHYLENE RESPONSE FACTOR* (*MfERF1*), and *AUXIN INDUCED IN ROOT CULTURE*, on cold tolerance have been documented (Guo et al., 2014; Zhuo et al., 2018; Wang et al., 2021). Two CMLs associated with abiotic stress responses have been investigated. *MtCML40* negatively regulates salt tolerance in *M. truncatula* although it is responsive to cold, salt, osmotic stress, and ABA (Zhang et al., 2019). *MtCML42* regulates cold tolerance and early flowering through upregulating the CBF pathway and downregulating *MtABI5*, respectively (Sun et al., 2021). However, the function of CMLs in alfalfa and their regulation on cold tolerance are still unknown.

At least one low-temperature-responsive element is observed in the promoter region of six *MtCML* genes, including *MtCML10* (Sun et al., 2020), implying that these *MtCMLs* are possibly involved in cold responses in *Medicago* plants. Given the important role of Ca^{2+} signaling in cold tolerance, the objective of this study was to study the regulation of *MsCML10* and its homolog *MtCML10* on cold tolerance. We documented that MsCML10 and MtCML10 could regulate cold tolerance through interactions with GST and fructose 1,6-biphosphate aldolase.

Results

Molecular characterization and spatial expression of *MsCML10*

The coding sequence of *MsCML10* and its homologous gene *MtCML10* were cloned from alfalfa and *M. truncatula*, respectively. *MsCML10* had an ORF (open reading frame) of 453 bp, encoding a peptide consisting of 150 amino acids (GenBank accession No. OM049783) with a molecular weight of 17.16 kDa. MsCML10 was 100% identical to MtCML10 in amino acid sequence and had 78.67% identity with AtCML11 in Arabidopsis. Phylogenetic tree analysis showed that MsCML10 was mostly close to AtCML11 in Arabidopsis (Supplemental Figure S1). Structural domain analysis using SMART (http://smart.embl-heidelberg.de/) showed that MsCML10 had four EF-hand motifs similar to MtCML10 and AtCML11 (Supplemental Figure S2).

Analysis of subcellular localization of MsCML10 showed that the MsCML10-GFP fluorescence was observed in cytoplasm and nucleus, while the fluorescence of GFP or nuclear localization marker control was observed throughout cell or in the nucleus, respectively (Figure 1A). The results indicated that MsCML10 was located in the cytoplasm and nucleus. The *MsCML10* transcript was detected in the roots, stems,

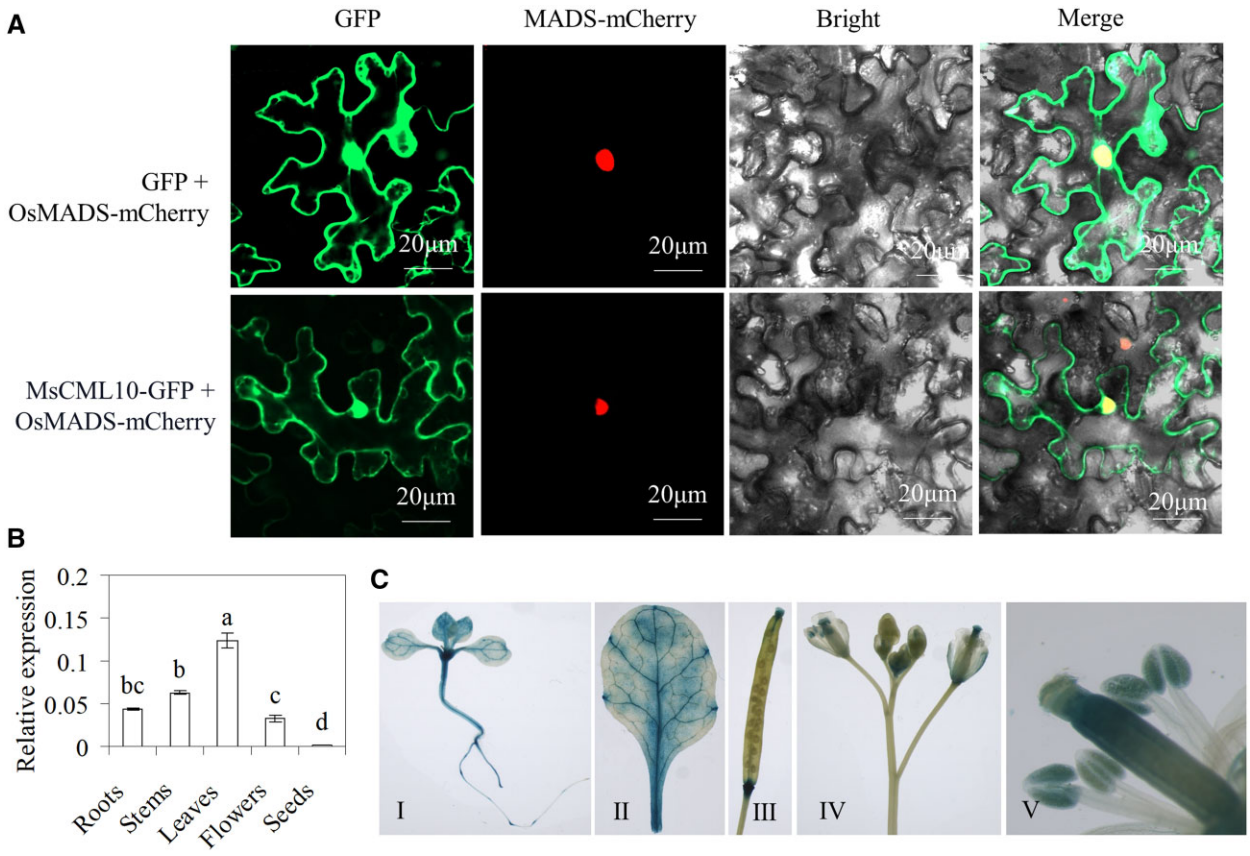

Figure 1 Subcellular localization of MsCML10 and the expression pattern. The vectors *MsCML10*::GFP or GFP in combination with mCherry-tagged MADS were co-transformed into *N. benthamiana* leaves for analysis of subcellular localization (A). Spatial expression of *MsCML10* in alfalfa was analyzed using RT–qPCR (B). Seedlings (I), leaflet (II), silique (III), flower (IV), and stamen (V) in $P_{MsCML10}$::GUS transgenic Arabidopsis was used for GUS staining (C). Means of three replicates and standard errors are presented; the same letter above the column indicates no significant difference at $P < 0.05$ using Duncan's test.

leaves, flowers, and seeds of alfalfa, with the highest level in leaves (Figure 1B). Transgenic Arabidopsis expressing the β-*glucuronidase* (*GUS*) reporter gene driven by a 1,500-bp promoter of *MsCML10* was generated. GUS staining results showed that GUS activity was observed in leaves, roots, anthers, stigma, and the ends of silique (Figure 1C), which is consistent with the *MsCML10* transcript detected in alfalfa (Figure 1B).

MsCML10 and its homolog *MtCML10* positively regulate cold tolerance in alfalfa and *M. truncatula*

MsCML10 and *MtCML10* were induced by cold treatment. The *MsCML10* transcript was greatly induced after 2–12 h of cold treatment, with the highest level (40-fold) at 6 h (Figure 2A), while the *MtCML10* transcript was induced after 2 to 12 h of cold treatment, with the highest level (10-fold) at 12 h (Figure 2B). In order to explore the role of *MsCML10* in regulating cold tolerance, transgenic alfalfa plants overexpressing *MsCML10* or downregulating *MsCML10* by RNAi were generated. Two overexpressing lines (OE1 and OE5) and two RNAi lines (RNAi2 and RNAi5) showing greatly increased or decreased *MsCML10* transcript levels were selected for further study (Figure 2, C and D).

CA treatment resulted in a decrease in the temperature resulted in 50% electrolyte leakage (TEL_{50}) and an increase in survival rate in all plant genotypes (Figure 3, A, B, and E), indicating that CA increased cold tolerance in alfalfa. Compared to the wild-type (WT), overexpression lines in alfalfa had lower levels of TEL_{50} and higher levels of survival rate, while RNAi lines had higher levels of TEL_{50} and lower levels of survival rate under both nonacclimated (NA) and CA conditions (Figure 3, A, B, and E). The results indicated that *MsCML10* positively regulates cold tolerance in alfalfa.

Transgenic *M. truncatula* plants overexpressing *MsCML10* were generated. Three transgenic lines (OE9, OE15, and OE22) showing greatly increased *MsCML10* transcript were selected (Figure 2E). Similar to alfalfa plants, CA treatment resulted in a decrease in TEL_{50} and an increase in survival rate in both transgenic lines and the WT plants (Figure 3, C, D, and F), while transgenic lines had lower levels of TEL_{50} and higher levels of survival rate than the WT under NA and CA conditions (Figure 3, C, D, and F). In addition, a homozygous mutation line with *Tnt1* retrotransposon insertion in the fourth exon of *MtCML10*, *cml10-1*, was identified (Supplemental Figure S3a). Compared to the WT, no *MtCML10* transcript was detected in *cml10-1* (Supplemental

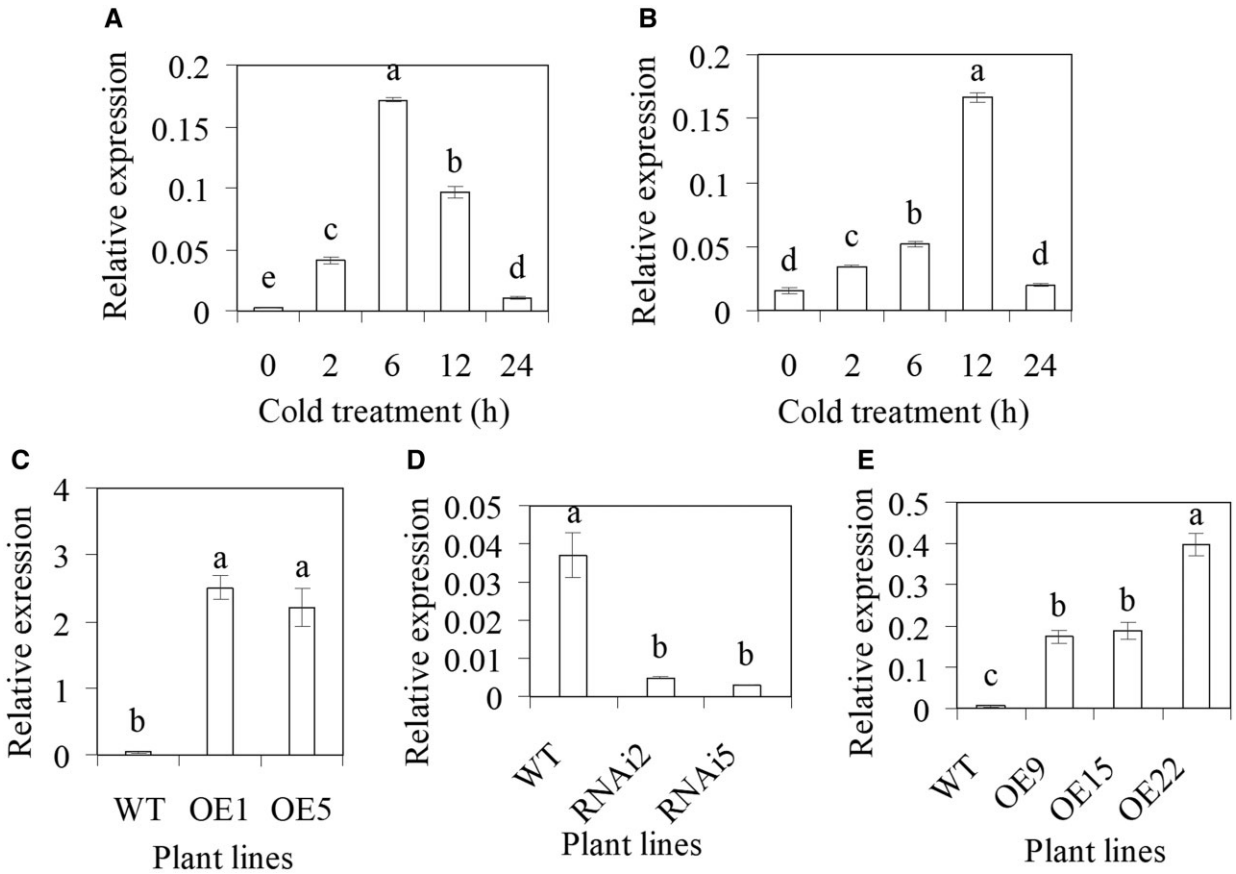

Figure 2 Analysis of transcript levels of *MsCML10* and *MtCML10* in response to cold and transgenic alfalfa and *M. truncatula* plants. Relative expression of *MsCML10* (A) and *MtCML10* (B) in response to cold treatment at 5°C was analyzed using RT–qPCR. Transcript levels of *MsCML10* were analyzed in transgenic alfalfa overexpressing *MsCML10* (C), RNAi (D), and in transgenic *M. truncatula* overexpressing *MsCML10* (E). Means of three replicates and standard errors are presented; the same letter above the column indicates no significant difference at $P < 0.05$ using Duncan's test.

Figure S3b). Higher TEL_{50} and lower survival rate were observed in *cml10-1* than in the WT under both NA and CA conditions (Supplemental Figure S3, c–e), indicating that *MtCML10* was essential for cold tolerance in *M. truncatula*. The complementary plants (*MsCML10::cml10-1*) with a similar or slightly higher level of *MsCML10* transcript as that in the WT were generated (Supplemental Figure S4a). The complementary plant had the similar level of TEL_{50} to that in the WT, but lower level was observed in complementing plant than in *cml10-1* (Supplemental Figure S4b). The results indicated that the defect in cold tolerance in *cml10-1* could be complemented by expressing *MsCML10*.

Ca^{2+}-dependent interaction of MsCML10 with MsGSTU8 and MsFBA6

For understanding how MsCML10 regulates cold tolerance, a yeast two-hybrid (Y2H) screen was performed to identify proteins that interact with MsCML10. Several interacting clones were isolated, among them are *MsGST8* and *MsFBA6*. To verify the interaction, the full length of CDS of *MsGST8* and *MsFBA6* was used for Y2H analysis. The results showed that MsGST8 and MsFBA6 possibly interact with MsCML10 (Figures 4, A and 5, A). The interactions were further confirmed by using bimolecular fluorescence complementation (BiFC), firefly luciferase complementation imaging (LCI), GST pull-down and co-immunoprecipitation (Co-IP) assays. Co-expression of MsCML10-cYFP and YFP_N-MsGSTU8 or YFP_N-MsFBA6 in *Nicotiana benthamiana* leaves resulted in a strong YFP fluorescence in the cytosol in BiFC assay, while no fluorescence was shown in the negative controls (Figures 4b and 5b). The results indicated that GSTU8 and FBA6 were cytoplasmic isozymes. MtGSTU8 protein is predicted to be localized in the cytoplasm (Hasan et al., 2021). Phylogenetic tree analysis showed that MsGSTU8 and MsFBA6 were mostly similar to AtGSTU19 (Supplemental Figure S5) and cytoplasmic FBAs in Arabidopsis, respectively (Supplemental Figure S6). The interactions were also observed in the LCI assay (Figures 4, C and 5, C). The pull-down assay showed that MsGSTU8 or MsFBA6 interacts with GST-MsCML10, but not with GST alone (Figures 4, D and 5, D). The interactions were further verified using Co-IP assay when MsGSTU8-GFP or MsFBA6-GFP was co-expressed with Flag-MsCML10 in leaf cells of *N. benthamiana*. Immunoblot analysis using an anti-Flag antibody showed that both MsGSTU8 and MsFBA6 interacted with MsCML10 (Figures 4, E and 5, E). The above results indicated that MsCML10 interacted with MsGST8 and MsFBA6.

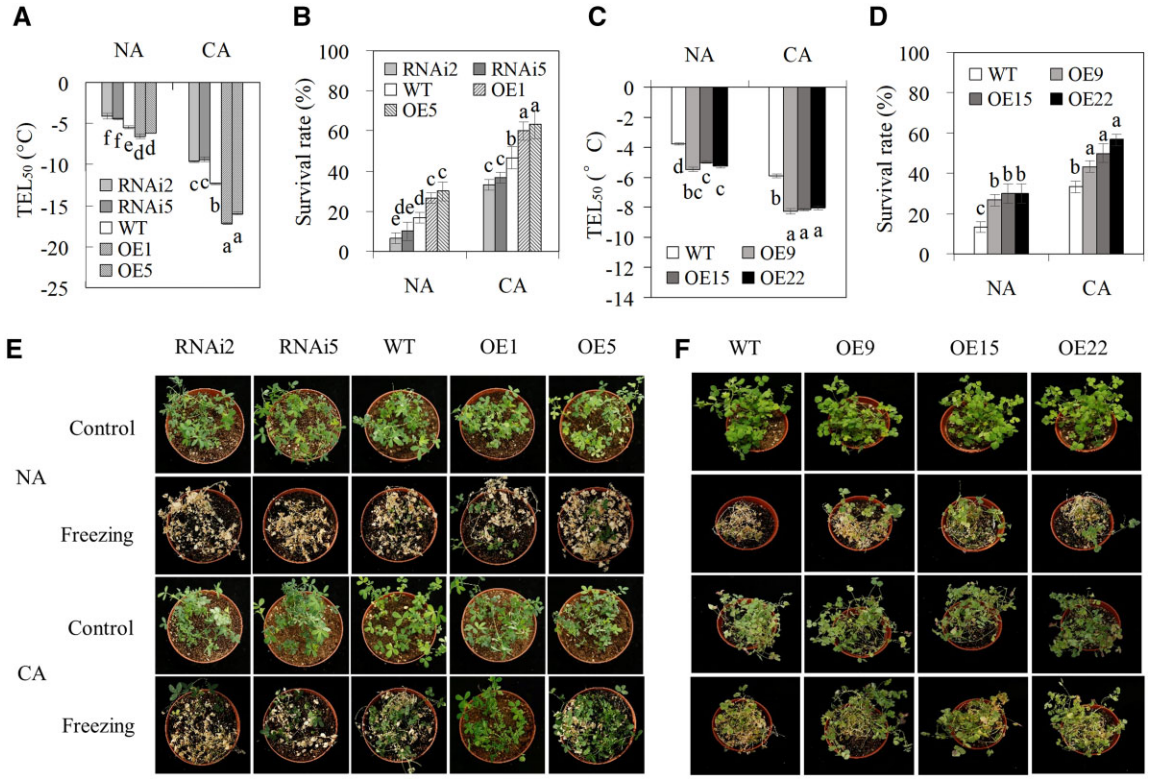

Figure 3 Analysis of cold tolerance in *MsCML10*-overexpressing and RNAi plants in comparison with the WT. The temperature resulting in TEL_{50} and survival rate in transgenic alfalfa and *M. truncatula* plants. Plants were placed in a growth chamber at 5°C for 7 days for CA treatment, while those at room temperature received the NA treatment. TEL_{50} was measured in *MsCML10*-RNAi and *MsCML10*-overexpressing alfalfa (A) as well as in *MsCML10*-overexpressing *M. truncatula* (C). Survival rates were measured after plants were treated by freezing at −5°C (NA plants) or −7°C (CA plants) for 6 h (B and D). After 2 days of recovery at room temperature, the freeze-treated and control alfalfa (E) and *M. truncatula* (F) plants were photographed. Means of three replicates and standard errors are presented; the same letter above the column indicates no significant difference at $P < 0.05$ using Duncan's test.

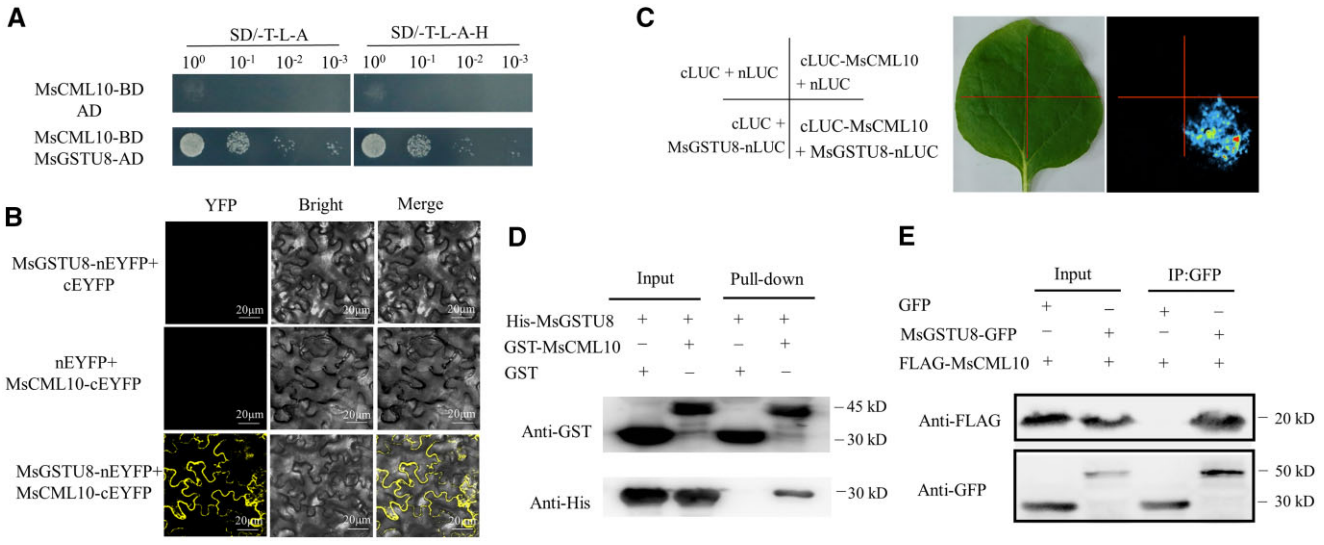

Figure 4 Analysis of interaction of MsCML10 with MsGSTU8. Interaction of MsCML10 with MsGSTU8 was analyzed using the methods of Y2H (A), BiFC (B), the LCI (C), pull-down (D), and Co-IP (E). GST-MsCML10 fusion protein was used as bait and His-MsGSTU8 fusion protein as prey in the pull-down assay. Anti-His and anti-GST antibodies were used to detect bait and prey proteins, and the His and GST proteins were used as negative controls (D). Flag-MsCML10 and MsGSTU8-GFP were co-expressed in leaves of *N. benthamiana*. Total proteins were subjected to immunoprecipitation with anti-GFP beads. The presence of Flag-MsCML10 was detected by anti-Flag immunoblotting (E).

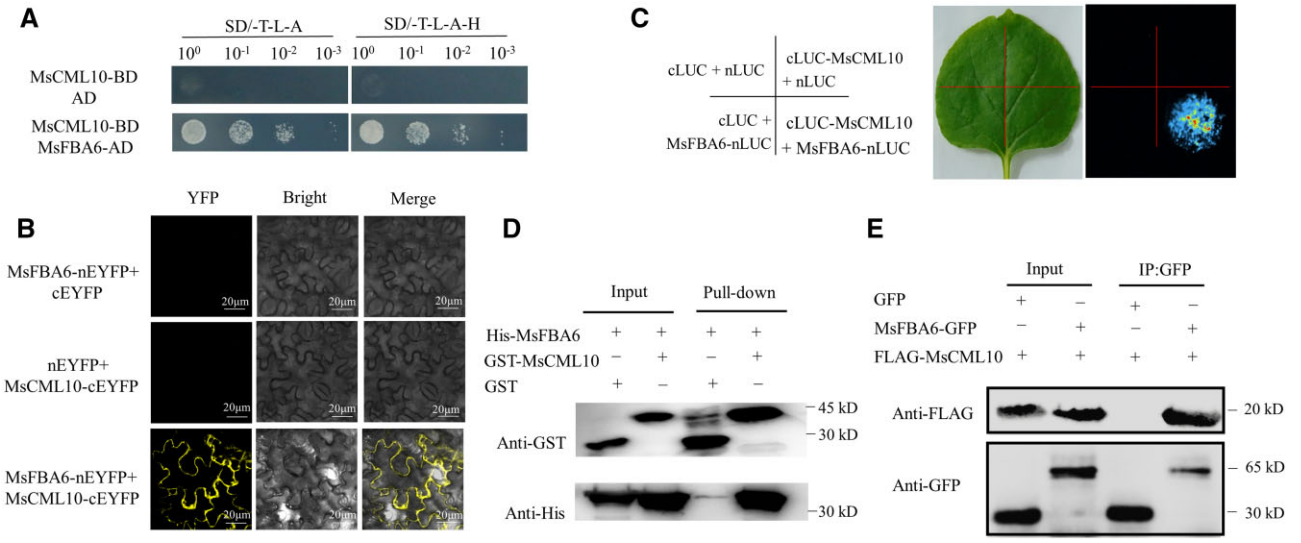

Figure 5 Analysis of interaction of MsCML10 with MsFBA6. Interaction of MsCML10 with MsFBA6 was analyzed using the methods of Y2H (A), BiFC (B), the LCI (C), pull-down (D), and Co-IP (E). GST-MsCML10 fusion protein was used as bait and His-MsFBA6 fusion protein as prey in the pull-down assay. Anti-His and anti-GST antibodies were used to detect bait and prey proteins, and the His and GST proteins were used as negative controls (D). Flag-MsCML10 and MsFBA6-GFP were co-expressed in leaves of *N. benthamiana*. Total proteins were subjected to immunoprecipitation with anti-GFP beads. The presence of Flag-MsCML10 was detected by anti-Flag immunoblotting (E).

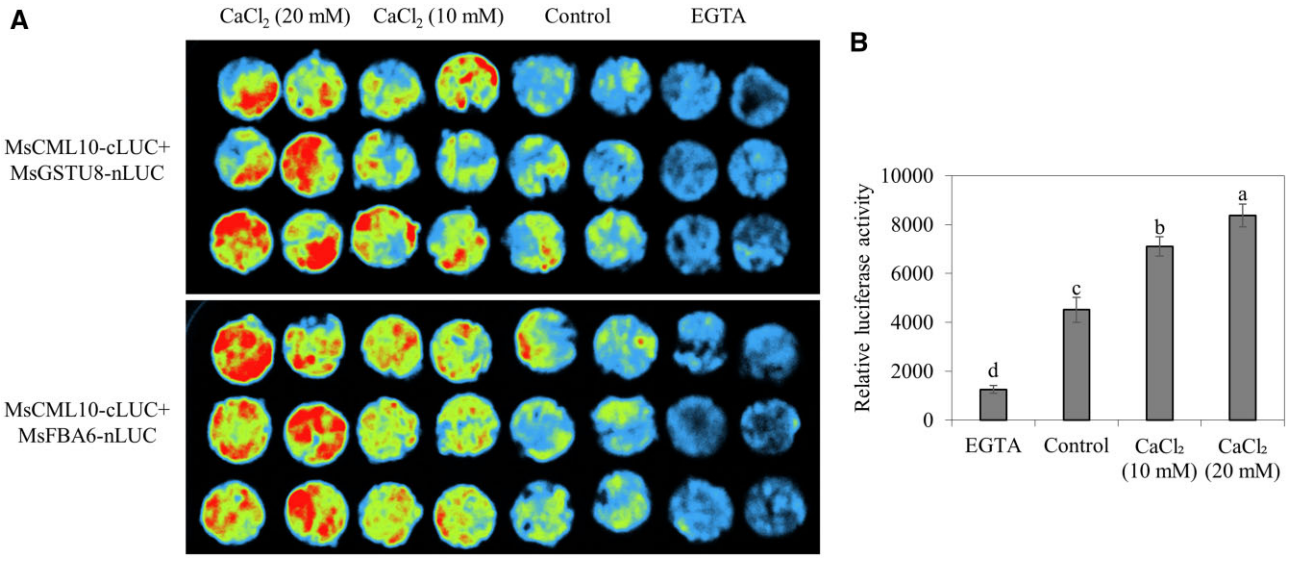

Figure 6 Analysis of Ca^{2+}-dependent interaction of MsCML10 with MsGSTU8 or MsFBA6. *Nicotiana benthamiana* leaves co-transformed using the mixed Agrobacterium harboring 35S::cLUC-MsCML10 and 35S::MsGSTU8-nLUC or 35S::MsFBA6-nLUC were placed on 4% agar containing 10- or 20-mM $CaCl_2$, 20-mM EGTA or without any supplement as control for 48 h, followed by capturing the luciferase image (A) or measuring the fluorescence intensity as the relative LUC activity (B). Means of the data from eight-leaf discs and standard errors are presented; the same letter above the column indicates no significant difference at $P < 0.05$ using Duncan's test.

To investigate whether of the interaction between MsCML10 and MsGSTU8 or MsFBA6 was dependent upon Ca^{2+}, a transient FLC assay was performed in the presence of $CaCl_2$ or EGTA. The results showed that $CaCl_2$-treated leaves had stronger interaction signal, while the EGTA-treated leaves had weaker signal as compared with the control (Figure 6, A and B), indicating that the interaction between MsCML10 and MsGSTU8 or MsFBA6 was dependent upon Ca^{2+}.

The GST activity and ROS level is affected by *MsCML10* expression

The GST activity was increased in all genotypes of alfalfa plants after cold treatment (Figure 7A). Compared to the WT, GST activity was higher in *MsCML10* overexpressing lines but lower in RNAi lines under both NA and CA conditions (Figure 7A). Likely, higher GST activity was observed in overexpressing lines in *M. truncatula*, but lower level in *cml10-1* was observed as compared with the WT under

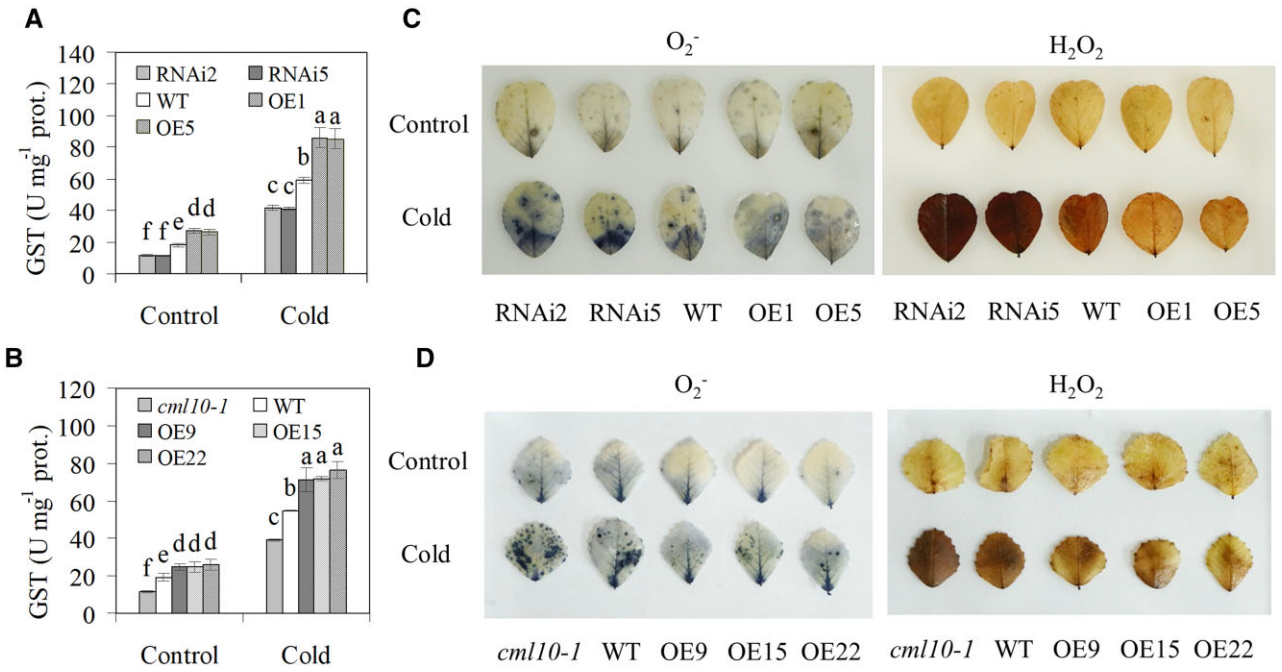

Figure 7 Analysis of GST activity and ROS levels in response to cold. GST activity in *MsCML10*-RNAi and *MsCML10*-overexpressing alfalfa (A) as well as in *MsCML10*-overexpressing *M. truncatula* and *cml10-1* (B) in comparison with the WT were measured after 7 days of cold treatment at 5°C. H_2O_2 and O_2^- in *MsCML10*-RNAi and *MsCML10*-overexpressing alfalfa (C) as well as in *MsCML10*-overexpressing *M. truncatula* and *cml10-1* (D) were measured after 7 days of cold treatment at 5°C. Means of three replicates and standard errors are presented; the same letter above the column indicates no significant difference at $P < 0.05$ using Duncan's test.

both NA and CA conditions (Figure 7B). ROS levels in the plants overexpressing and RNAi lines were examined. Leaves in overexpressing lines were less stained by 3,3-diaminobenzidine (DAB) and nitroblue tetrazolium (NBT) than WT plants, while the staining was substantially stronger in the RNAi lines (Figure 7C). Similar results were also shown in overexpressing lines in *M. truncatula* and *cml10-1* (Figure 7D). The results indicated that lower levels of ROS (H_2O_2 and O_2^-) in overexpressing lines and higher level in RNAi and *cml10-1* lines were accumulated as compared with the WT after CA treatment.

The FBA activity and sugar accumulation is affected by *MsCML10* expression

Fructose 1,6-bisphosphate aldolase activity was increased in all genotypes of alfalfa and *M. truncatula* plants after CA treatment (Figure 8, A and E). Compared to the WT, FBA activity was higher in overexpressing alfalfa and *M. truncatula* lines and lower in alfalfa RNAi lines and *cml10-1* under both NA and CA conditions (Figure 8, A and E). Soluble sugars (sucrose, glucose, and fructose) levels showed the similar alterations with FBA activity in the different genotypes of plants (Figure 8, B–D and F–H). The results indicated that the alterations in sugars were associated with the altered FBA activity.

Discussion

A transient increase in cytosolic Ca^{2+} concentration is common in plants in response to abiotic stress. The Ca^{2+} signal is decoded by Ca^{2+} sensors including CaM, CML, CBL, and CDPK through activating interaction proteins and regulating downstream cellular responses (Lecourieux et al., 2006). MsCML10 from alfalfa was characterized in the present study. It is identical to MtCML10 in amino acid sequence and mostly similar to AtCML11 in Arabidopsis. EF-hand motifs are the sites binding with Ca^{2+}, which is the conserved domain in Ca^{2+}-binding proteins (Reddy et al., 2011). One to four EF-hand motifs are present in MtCMLs in *M. truncatula* (Sun et al., 2020). Four EF-hand motifs were observed in MsCML10. In addition, MsCML10 was located in the cytoplasm and nucleus, although no nuclear signal peptide was observed in the MsCML10 sequence. The fused MsCML10-GFP is still small (~44.16 kDa); thus, it is presumed that MsCML10 was localized in the cytoplasm, but it may diffuse nonspecifically into nucleus through nuclear pores like MtCML42 (Sun et al., 2021).

Although some *CML* members are responsive to abiotic stresses in Arabidopsis (Magnan et al., 2008; Vadassery et al., 2012; Scholz et al., 2015; Wu et al., 2017), their role in regulation of cold tolerance has not been documented. Similar to *MtCML42* in *M. truncatula* (Sun et al., 2021), *MsCML10* and *MtCML10* transcripts were greatly induced by cold, while the induction of *MsCML10* was earlier with a higher level than that of *MtCML10*. Overexpression of *MsCML10* resulted in enhanced cold tolerance in alfalfa and *M. truncatula*, while downregulating *MsCML10* and mutation of *MtCML10* resulted in decreased cold tolerance in alfalfa RNAi lines and *cml10-1*, respectively. In addition, the defect in cold

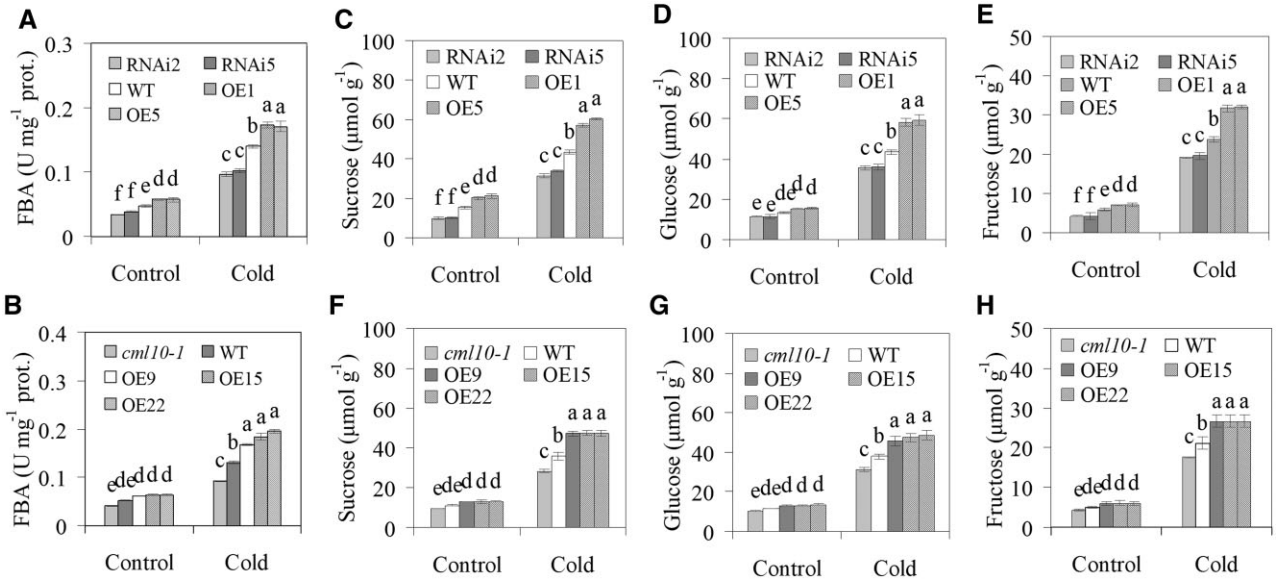

Figure 8 Analysis of FBA activity and sugar concentrations in response to cold. FBA activity in *MsCML10*-RNAi and *MsCML10*-overexpressing alfalfa (A) as well as in *MsCML10*-overexpressing *M. truncatula* and *cml10-1* (B) in comparison with the WT were measured after 7 days of cold treatment at 4°C. Sucrose (C and F), glucose (D and G), and fructose (E and H) in *MsCML10*-RNAi and *MsCML10*-overexpressing alfalfa (C, D, and E) as well as in *MsCML10*-overexpressing *M. truncatula* and *cml10-1* (F, G, and H) were measured after 7 days of cold treatment at 4°C. Means of three replicates and standard errors are presented; the same letter above the column indicates no significant difference at $P < 0.05$ using Duncan's test.

tolerance in *cml10-1* was complemented by expressing *MsCML10*. The results suggest that MsCML10 and MtCML10 positively regulate cold tolerance in alfalfa and *M. truncatula*. MtCML42 regulates cold tolerance through upregulating the CBF pathway and *MtGolS* expression for increased RFO accumulation in *M. truncatula* (Sun et al., 2021).

MsGSTU8 was documented to interact with MsCML10 and the interaction is dependent upon Ca^{2+}. GSTU is a plant-specific GST that plays a key role in ROS scavenging (Xu et al., 2016). GSTU19 confers multiple tolerance to salt, drought and methyl viologen-induced oxidative stress in Arabidopsis (Xu et al., 2016). GSTU can be activated by phytohormone signaling. TaGST1 is activated by BRASSINAZOLE-RESISTANT 2 for regulation of drought tolerance in wheat (*Triticum aestivum*; Cui et al., 2019). *PtrGSTU17* expression is regulated by ERF9 for regulation of cold tolerance by maintaining ROS homeostasis in *Poncirus trifoliata* (Zhang et al., 2022). GST activity was increased in all genotypes of plants and a higher level was obtained in *MsCML10* overexpressing alfalfa and *M. truncatula* and lower level was in RNAi alfalfa and *cml10-1* mutant as compared with the WT after CA treatment. In addition, lower levels of ROS (H_2O_2 and $O_2^{\cdot-}$) were observed in overexpressing lines of *MsCML10*, while higher levels were in the RNAi lines and *cml10-1* mutant than in the WT, suggesting that the altered ROS levels were associated with GST activity and *MsCML10* and *MtCML10* transcript levels. ROS production is unavoidable under low temperature as a result of inhibition of the Calvin–Benson cycle enzyme activity that limits the use of absorbed light energy by CO_2 assimilation (Suzuki et al., 2012). Thus, ROS homeostasis is important for plant CA. Our results suggest that MsCML10 regulates cold tolerance by activating MsGSTU8 to maintain ROS homeostasis.

Interaction of MsCML10 with MsFBA6 was observed in cytosol and depended upon the presence of Ca^{2+}. The interaction localization and similarity of MsFBA6 with Arabidopsis cytoplasmic FBAs suggest that MsFBA6 is a cytoplasmic isozyme. FBA activity was increased in all plants after CA treatment, and higher activity of FBA was observed in *MsCML10* overexpressing alfalfa and *M. truncatula* plants, while lower activity was in RNAi and *cml10-1* plants, suggesting that FBA activity was activated by MsCML10 or MtCML10 in alfalfa and *M. truncatula*. Cytoplasmic FBA catalyzes the reversible conversion of fructose-1,6-diphosphate (FBP) into dihydroxyacetone phosphate and glyceraldehyde-3-phosphate during glycolysis and gluconeogenesis and is involved in sugar metabolism (Ronimus and Morgan, 2003). Sugar accumulation plays an important role in winter hardening in alfalfa (Cunningham et al., 2001; Seppanen et al., 2018) and in cold tolerance in *M. truncatula* (Zhang et al., 2011). Sucrose, glucose, and fructose concentrations were increased after cold treatment in alfalfa and *M. truncatula* plants, with higher levels in *MsCML10* overexpressing plants but lower levels in RNAi and *cml10-1* plants. The altered sugar concentrations were associated with changes in FBA activity. Transgenic tomato plants overexpressing *SiFBA5* from *Saussurea involucrata* show increased cold tolerance and biomass (Mu et al., 2021). Overexpression of *FBA7* results in increased net photosynthetic rate and stem thickness in *N. benthamian* plants (Cai et al., 2016). Nevertheless, our results suggest that interaction of MsCML10 with MsFBA6 resulted in accumulated sugars that was associated

with the increased cold tolerance in alfalfa and *M. truncatula* plants.

Conclusions

MsCML10 and *MtCML10* transcripts were induced in response to cold. Upregulation or downregulation of *MsCML10* resulted in increased or decreased cold tolerance, respectively, while *cml10-1* showed decreased cold tolerance that could be complemented by expressing *MsCML10*. The Ca^{2+}-dependent interaction of MsCML10 with MsGSTU8 and MsFBA6 and the altered activities of GST and FBA and levels of ROS and sugars were associated with the *MsCML10* transcript level. It is suggested that MsCML10 decodes the cold-induced Ca^{2+} signal and regulates cold tolerance through activating MsGSTU8 and MsFBA6, which leads to maintaining ROS homeostasis and increased accumulation of sugars for osmoregulation, respectively.

Materials and methods

Plant growth and stress treatments

A *Tnt1* retrotransposon inserted mutant (NF19519) was obtained from the Noble Research Institute (https://medicago-mutant.noble.org/mutant/) for selecting homozygous line *cml10-1* using retrotransposon display PCR as described (Tadege et al., 2008). Alfalfa (*M. sativa* L. cv. Regen-SY4D), *M truncatula* cv. R108 and *cml10-1*, as well as the transgenic plants, were grown in plastic pots of 15 cm in diameter in a greenhouse at 25°C under natural light, as described previously (Sun et al., 2021). Alfalfa was placed in a growth chamber at 5°C under 14 h of light for cold treatment and used to isolate total RNA. Sterilized seeds of Arabidopsis (*A. thaliana*) and *N. benthamiana* were placed on 1/2 MS medium for germination at 24°C for 7 days, and the seedlings were transplanted to a mixture of peat and perlite (3:1, v/v) and grown in a growth chamber at 22°C under 14 h of light for 3–4 weeks.

Isolation of total RNA and analysis of reverse transcription quantitative PCR and RT–PCR

Total RNA was isolated using the RNAprep Pure Plant Kit (Tiangen, Beijing, China), and 1 μg RNA was used for synthesis of the first strand cDNA using the TaKaRa PrimeScript RT kit with gDNA Eraser according to the manufacturer's protocol. Reverse transcription–quantitative PCR (RT–qPCR) was conducted using Thermal Cycler Dice Real Time System II (Takara, Shiga, Japan) with three biological replicates of independent samples. The RT–qPCR solution (10 μL) contained 0.2-μM forward primer and reverse primer, 200-ng cDNA, and 5-μL SYBR qPCR master mix. The RT–qPCR solution (50 μL) contained 0.2-μM forward primer and reverse primer, 200-ng cDNA, 1 μL Ex Taq DNA polymerase, and 5-μL deoxyribonucleotide triphosphate (Takara, Dalian, China). The *MsActin* and *MtActin7* (*Medtr3g095530*) genes that showed 100% identity in nucleic acid sequence were used as the internal controls. Relative expression was calculated using the normalized ($2^{-\Delta\Delta Ct}$) value. The primers used for RT–qPCR and RT–PCR analysis are listed in Supplemental Table S1. DNAMAN software (Lynnon Biosoft, Vaudreuil, Quebec, Canada) was used for analysis of amino acid sequence.

Analysis of subcellular localization of MsCML10

The coding sequence of *MsCML10* without stop codon was cloned into the vector pCAMBIA-1305 and fused with GFP driven by CaMV 35S promoter. The construct (35S::*MsCML10*-GFP) or the control vector (35S::GFP) in combination with 35S:*OsMADS*-mCherry vector were used to co-transform leaves of 1-month-old *N. benthamiana* plants using the *Agrobacterium tumefaciens*-mediated transformation method (Kumar and Kirti, 2010). The plants were incubated at 25°C for 72 h in a growth chamber, and the transformed leaves were observed and photographed using a confocal laser scanning microscope (Zeiss LSM800, Germany), using excitation/emission wavelengths 488/498–540 nm for GFP and 552/600–640 nm for mCherry.

Generation of transgenic plants

The coding sequence of *MsCML10* driven by the CaMV 35S promoter was cloned into the pCAMBIA3301 binary expression vector (35S::*MsCML10*). To construct a complementing vector ($P_{MtCML10}$::*MsCML10*), a 1,500-bp promoter of *MtCML10* upstream initiation codon was used to drive *MsCML10* in the binary expression vector pCAMBIA3301. To construct a RNAi vector, the sense fragment of *MsCML10* was constructed on the pFGC5941 vector using the XhoI and NcoI sites (Kerschen et al., 2004), and a 201-bp of antisense fragment was further cloned into the above vector using the SmaI and BamHI sites. Transgenic alfalfa or *M. truncatula* plants were generated using *A. tumefaciens* strain EHA105 containing the above vectors (Sun et al., 2021). For investigation of spatial expression, a 1,500-bp promoter of *MsCML10* upstream initiation codon (https://medicagohapmap2.org/) was used to drive *GUS* in the binary expression vector pCAMBIA3301. The *A. tumefaciens* strain EHA105 containing the above vector ($P_{MsCML10}$::GUS) was used to transform the WT Arabidopsis (Col0) by the method of floral dip.

GUS staining

The seedlings and a specific organ were immersed in GUS staining solution consisting of 50-mM sodium phosphate buffer (pH 7.2), 2-mM X-Gluc, 2-mM $K_4Fe(CN)_6$, 10-mM EDTA, 2-mM $K_3Fe(CN)_6$, and 0.1% (v/v) Triton X-100, with 30 min of vacuum. After incubating overnight at 37°C in the dark, the green tissues were decolorized in 70% (v/v) ethanol to remove chlorophyll for photography.

Evaluation of cold tolerance

Cold tolerance was evaluated based on survival rate and the temperature resulting in TEL_{50}. Two-month-old alfalfa and *M. truncatula* plants were placed in a growth chamber for 7 days of CA at 5°C or at room temperature as NA control. TEL_{50} was measured based on ion leakage of leaflets after

1 h of treatment at freezing temperatures and calculated by a fitted mode plot (Geng et al., 2021). For measurement of survival rate, 1-month-old plants were placed in a growth chamber with temperatures decreasing from 25°C to −5°C for NA plants or to −7°C for CA plants linearly within 6 h and maintained for 6 h, followed by moving to a fridge at 4°C overnight and then at room temperature for 2 days of recovery. The surviving seedlings were counted to calculate survival rate. The experiments consisted of three pots as repeats, and each pot contained seven individual plants.

Y2H assay

The Y2H assay was conducted using Matchmaker Gold Y2H System (Clontech, Mountain View, CA, USA) according to the manufacturer's instructions. The coding sequence of *MsCML10* was cloned into the pGBKT7 vector as a bait that was then transformed into the yeast strain Y2HGold. The transformed Y2HGold yeast strain was then transformed with the alfalfa cDNA library and placed on the synthetic dropout (SD) medium−Trp−Leu−Ade containing 10-mM 3-AT for selection at 30°C. Positive clones were selected for sequencing. The interactions between MsCML10 and MsGSTU8 or MsFBA6 were verified by Y2H assay as described above. The coding sequence of *MsGSTU8* and *MsFBA6* was inserted into the pGADT7 vector to produce the prey constructs. The prey vectors pGADT7-*MsGSTU8* or pGADT7-*MsFBA6* were transformed into the Y2HGold yeast strain expressing bait. The yeast cells were placed on SD medium−Trp−Leu−Ade−His containing 10 mM 3-AT for selection as above.

BiFC assay

The coding sequence of *MsCML10* without stop codon was fused with EYFP on the vector P2YC, while *MsGSTU8* or *MsFBA6* were fused with EYFP at the N-terminal of MsGSTU8 or MsFBA6 on vector P2YN, respectively. *Agrobacterium tumefaciens* containing MsCML10-cYFP and nYFP-MsGSTU8 or nYFP-MsFBA6 were used to co-transform the leaves of 1-month-old *N. benthamiana*, separately. Fluorescence of YFP was observed and photographed under a confocal laser scanning microscope (Zeiss LSM800, Germany), using excitation/emission wavelength 510 nm.

Firefly LCI analysis

The coding sequence of *MsCML10* was fused with cLUC on the vector pCAMBIA-cLUC, while *MsGSTU8* or *MsFBA6* was fused with nLUC on the vector pCAMBIA-nLUC (Ding et al., 2021). *Agrobacterium tumefasciens* GV3101 harboring 35S::cLUC-MsCML10 and 35S::MsGSTU8-nLUC or 35S::MsFBA6-nLUC were used to co-transform leaves of 1-month-old *N. benthamiana* plants (Pandey et al., 2015). For determination of Ca^{2+} dependence of the interaction, leaf discs of *N. benthamiana* were co-transformed using the above *Agrobacterium* strain and placed on 4% (w/v) agar containing 20-mM EGTA, 10-mM or 20-mM $CaCl_2$, or without any supplement as control for 48 h. The leaf discs were used to capture the luciferase image (Lumazone Pylon 2048B, Princeton, USA; Ding et al., 2021), or placed in a 96-well microtiter plate containing 200 µL of 1-mM fluorescein for 10 min to measure the fluorescence intensity as the relative LUC activity.

Pull-down assay

The coding sequence of *MsCML10* was cloned into pGEX-4T-1, while *MsGSTU8* and *MsFBA6* were cloned into pET-30a, separately. The GST-tagged MsCML10 and His-tagged MsGSTU8 or MsFBA6 protein was expressed and purified using columns packed with GST-agarose beads (Sangon Biotech, Shanghai, China) and a Ni-NTA Resin column (TransGen Biotech, Beijing, China), respectively, according to the manufacturer's instructions. The pull-down assay was performed as described by Zhang et al. (2016). GST-tagged MsCML10 or GST was immobilized on GST beads which were then suspended in Lysing buffer (150-mM NaCl, 10% (v/v) glycerol, 100-mM Tris−HCl, pH 7.5), and the same amount of MsGSTU8-His or MsFBA6-His protein was added. The mixture was rotated and incubated for 2 h at 4°C, followed by centrifugation for 1 min at 5,000*g* at 4°C. The pellet was washed 5 times with Lysing buffer and resuspended in 50 µL of 2× SDS protein electrophoresis loading buffer. A 10-µL sample was loaded on 10% (w/v) SDS−PAGE gel for electrophoresis, followed by transferring onto PVDF membrane (Millipore, Bedford, MA, USA). Immunoblotting was conducted using anti-GST or anti-His antibody.

Co-IP assay

Co-IP assay was performed as described by Zhu et al. (2022). The full-length CDS fragment of CML10 and the coding sequences of GSTU8 and FBA6 without stop codon were cloned, respectively, into the vector pCAMBIA-1305 harboring *35S:3×FLAG* or *35S:GFP* to obtain the recombinant constructs of FLAG-CML10, GSTU8-GFP and FBA6-GFP. The *A. tumefaciens* strain GV3101 harboring the Flag-CML10 and GSTU8-GFP or FBA6-GFP constructs was used to co-transform leaves of 4-week-old *N. benthamiana* plants. After 48 h, total protein was extracted from the transformed leaves using NB1 buffer containing 50 mM Tris−MES buffer (pH 8.0), 0.5-M sucrose, 1-mM $MgCl_2$, 10-mM EDTA, 5-mM DTT, and protease inhibitors, followed by incubating with anti-GFP antibody and magnetic beads for 2 h at 4°C with rotation. After three washes using wash buffer, the protein was eluted by boiling the beads with SDS buffer. Immunoprecipitated proteins were analyzed using SDS−PAGE and immunoblotted with anti-GFP or anti-Flag antibody.

Measurements of enzyme activities

Fresh leaves (0.1 g) were frozen in liquid nitrogen and grinded in 1 ml of 100-mM phosphate buffer (PBS) containing 1-mM GSH (pH 6.5), followed by centrifugation at 12,000*g* for 20 min at 4°C. The supernatants were collected for measurement of GST activity (Xu et al., 2016). The reaction solution (1 mL) contained 50-mM PBS (pH 7.4), 1-mM GSH, 0.5-mM 1-chloro-2, 4-Dinitrobenzene (CDNB), and

0.1-mL enzyme extract. The reaction was initiated by adding CDNB, and changes in absorbance at 340 nm within 1 min at 25°C were recorded to calculate GST activity based on the extinction coefficient of CDNB (9.6 $mM^{-1}\cdot cm^{-1}$). For extraction of FBA, fresh leaves (0.25 g) were ground in a mortar with a pestle in 3-mL precooled extraction buffer containing 50-mM KH_2PO_4 buffer (pH 7.0), 10% (v/v) glycerol, 4-mM $MgCl_2$, 1-mM EDTA, and 5-mM dithiothreitol. After centrifugation at 12,000*g* for 20 min at 4°C, the supernatants were used to determine FBA activity (Kamies et al., 2017). The reaction solution (1 mL) contained 50-mM HEPES–KOH buffer (pH 7.3), 1-mM EDTA, 0.1-mM NADH, 0.75 units of glycerol-3-phosphate dehydrogenase, 10 units of phosphotriose isomerase, and 100 µL of enzyme extract. The reaction was initiated by adding 0.1 mL of 4-mM FBP. The decrease in absorbance at 340 nm due to NADH oxidation within one minute at 25°C was recorded to calculate enzyme activity based on the extinction coefficient of NADH (6.22 $mM^{-1}\cdot cm^{-1}$). One unit of enzyme activity was defined as the amount of enzyme required for catalyzing the conversion of 1 µmol substrate within one minute. Protein concentration was determined using Coomassie Brilliant Blue G-250 (Bradford, 1976).

DAB and NBT staining

The leaflets detached from 2-month-old plants were immersed in DAB solution (1 mg mL^{-1}) for 1 h to detect H_2O_2 or in NBT solution (5 mg mL^{-1}) for 12 h in the dark to detect $O_2^{\cdot-}$ (Gou et al., 2020). The leaflets were decolorized in 95% (v/v) ethanol to remove chlorophyll for photography.

Measurements of soluble sugars

Fresh leaves (0.5 g) were frozen in liquid nitrogen and ground into a powder with addition of 5 mL of 80% (v/v) ethanol for extraction in a water bath at 80°C for 30 min. The mixture was cooled at room temperature and centrifuged at 12,000*g* for 20 min. The supernatant was quickly frozen in liquid nitrogen and vacuum-dried, followed by dissolving in 500 µL of deionized water and passing through a 0.22-µm Millipore membrane (Millipore, Bedford, MA, USA). The filtrate (30 µL) was injected into a Waters 2695 separation system, supplied with an amino bonded column (Zorbax NH2; 250 × 4.6 mm; Agilent Technologies Inc., Santa Clara, CA, USA) and Waters 2414 refractive index detector. The sugar concentration was calculated based on the standard curve for each sugar and calibrated according to the recovery throughout the analysis procedure (Sun et al., 2021).

Statistical analysis

The physiological measurements were repeated 3 times from different plant samples. All data were subjected to analysis of variances according to the model for completely randomized design using an SPSS program (SPSS Inc., Chicago, IL, USA). Differences among means of treatments and plant lines were evaluated using Duncan's test at 0.05 probability level.

Data Availability Statement

The data that support the findings of this study are available from the corresponding author upon reasonable request.

Accession numbers

Sequence data from this article can be found in the GenBank/EMBL data libraries under accession numbers (OM049783).

Supplemental data

The following materials are available in the online version of this article.

Supplemental Figure S1. Phylogenetic tree of MsCML10 and 50 AtCMLs.

Supplemental Figure S2. Multiple alignment of MsCML10 with MtCML10 and AtCML11.

Supplemental Figure S3. Analysis of cold tolerance in *cml10-1* plants in comparison with the WT.

Supplemental Figure S4. Analysis of the complementary plants as compared with the *cml42* mutant and the WT.

Supplemental Figure S5. Phylogenetic tree of MsGSTU8 and AtGSTs.

Supplemental Figure S6. Phylogenetic tree of MsFBA6 and AtFBAs.

Supplemental Table S1. Primer sequences used for RT–qPCR and RT–PCR and the accession numbers of the analyzed genes.

Funding

This work was supported by the National Natural Science Foundation of China (Grant number: 32030074).

Conflict of interest statement. None declared.

References

Astegno A, Bonza MC, Vallone R, La Verde V, D'Onofrio M, Luoni L, Molesini B, Dominici P (2017) *Arabidopsis* calmodulin-like protein CML36 is a calcium (Ca^{2+}) sensor that interacts with the plasma membrane Ca^{2+}-ATPase isoform ACA8 and stimulates its activity. J Biol Chem **292**: 15049–15061

Cai BB, Li Q, Xu YC, Yang L, Bi HG, Ai XZ (2016) Genome-wide analysis of the fructose 1,6-bisphosphate aldolase (FBA) gene family and functional characterization of FBA7 in tomato. Plant Physiol Biochem **108**: 251–265

Campos WF, Dressano K, Ceciliato PHO, Guerrero-Abad JC, Silva AL, Fiori CS, do Canto AM, Bergonci T, Claus LAN, Silva-Filho MC, et al. (2018) *Arabidopsis thaliana* rapid alkalinization factor 1-mediated root growth inhibition is dependent on calmodulin-like protein 38. J Biol Chem **293**: 2159–2171

Castonguay Y, Bertrand A, Michaud R, Laberge S (2011) Cold-induced biochemical and molecular changes in alfalfa populations selectively improved for freezing tolerance. Crop Sci **51**: 2132–2144

Cheng HQ, Han LB, Yang CL, Wu XM, Zhong NQ, Wu JH, Wang FX, Wang HY, Xia GX (2016) The cotton MYB108 forms a positive feedback regulation loop with CML11 and participates in the defense response against *Verticillium dahliae* infection. J Exp Bot **67**: 1935–1950

Chiasson D, Ekengren SK, Martin GB, Dobney SL, Snedden WA (2005) Calmodulin-like proteins from *Arabidopsis* and tomato are involved in host defense against *Pseudomonas syringae pv.* tomato. Plant Mol Biol **58**: 887–897

Cho KM, Nguyen HTK, Kim SY, Shin JS, Cho DH, Hong SB, Shin JS, Ok SH (2016) CML10, a variant of calmodulin, modulates ascorbic acid synthesis. New Phytol **209**: 664–678

Cui XY, Gao Y, Guo J, Yu TF, Zheng WJ, Liu YW, Chen J, Xu ZS, Ma YZ (2019) BES/BZR transcription factor TaBZR2 positively regulates drought responses by activation of TaGST1. Plant Physiol **180**: 605–620

Cunningham SM, Gana JA, Volenec JJ, Teuber LR (2001) Winter hardiness, root physiology, and gene expression in successive fall dormancy selections from 'Mesilla' and 'CUF 101' alfalfa. Crop Sci **41**: 1091–1098

Ding L, Wu Z, Teng R, Xu S, Cao X, Yuan G, Zhang D, Teng N (2021) LlWRKY39 is involved in thermotolerance by activating LlMBF1c and interacting with LlCaM3 in lily (*Lilium longiflorum*). Hortic Res **8**: 36

Ding YL, Shi YT, Yang SH (2019) Advances and challenges in uncovering cold tolerance regulatory mechanisms in plants. New Phytol **222**: 1690–1704

Geng B, Wang Q, Huang R, Liu Y, Guo Z, Lu S (2021) A novel LRR-RLK (CTLK) confers cold tolerance through regulation on the C-repeat-binding factor pathway, antioxidants, and proline accumulation. Plant J **108**: 1679–1689

Gou L, Zhuo C, Lu S, Guo Z (2020) A universal stress protein from *Medicago falcata* (*MfUSP1*) confers multiple stress tolerance by regulating antioxidant defense and proline accumulation. Environ Exp Bot **178**: 104168

Guo Z, Tan J, Zhuo C, Wang C, Xiang X, Wang Z (2014) Abscisic acid, H_2O_2 and nitric oxide interactions mediated cold-induced S-adenosylmethionine synthetase in *Medicago sativa* subsp. *falcata* that confers cold tolerance through up-regulating polyamine oxidation. Plant Biotechn J **12**: 601–612

Hasan MS, Singh V, Islam S, Islam MS, Ahsan R, Kaundal A, Islam T, Ghosh A (2021) Genome-wide identification and expression profiling of glutathione S-transferase family under multiple abiotic and biotic stresses in *Medicago truncatula L*. PLoS One **16**: e0247170

Kamies R, Farrant JM, Tadele Z, Cannarozzi G, Rafudeen MS (2017) A proteomic approach to investigate the drought response in the orphan crop *Eragrostis tef*. Proteomes **5**: 32

Kerschen A, Napoli CA, Jorgensen RA, Muller AE (2004) Effectiveness of RNA interference in transgenic plants. FEBS Lett **566**: 223–228

Kumar KRR, Kirti PB (2010) A mitogen-activated protein kinase, AhMPK6 from peanut localizes to the nucleus and also induces defense responses upon transient expression in tobacco. Plant Physiol Biochem **48**: 481–486

Leba LJ, Cheval C, Ortiz-Martin I, Ranty B, Beuzon CR, Galaud JP, Aldon D (2012) CML9, an *Arabidopsis* calmodulin-like protein, contributes to plant innate immunity through a flagellin-dependent signalling pathway. Plant J **71**: 976–989

Lecourieux D, Raneva R, Pugin A (2006) Calcium in plant defence-signalling pathways. New Phytol **171**: 249–269

Ma Q, Zhou Q, Chen C, Cui Q, Zhao Y, Wang K, Arkorful E, Chen X, Sun K, Li X (2019) Isolation and expression analysis of CsCML genes in response to abiotic stresses in the tea plant (*Camellia sinensis*). Sci Rep **9**: 8211

Ma W, Smigel A, Tsai YC, Braam J, Berkowitz GA (2008) Innate immunity signaling: cytosolic Ca^{2+} elevation as an early signal is linked to downstream nitric oxide generation through the action of calmodulin or a calmodulin-like protein. Plant Physiol **148**: 818–828

Magnan F, Ranty B, Charpenteau M, Sotta B, Galaud JP, Aldon D (2008) Mutations in AtCML9, a calmodulin-like protein from *Arabidopsis thaliana*, alter plant responses to abiotic stress and abscisic acid. Plant J **56**: 575–589

Midhat U, Ting MKY, Teresinski HJ, Snedden WA (2018) The calmodulin-like protein, CML39, is involved in regulating seed development, germination, and fruit development in *Arabidopsis*. Plant Mol Biol **96**: 375–392

Mu J, Fu Y, Liu B, Zhang Y, Wang A, Li Y, Zhu J (2021) SiFBA5, a cold-responsive factor from *Saussurea involucrata* promotes cold resilience and biomass increase in transgenic tomato plants under cold stress. BMC Plant Biol **21**: 75

Munir S, Liu H, Xing Y, Hussain S, Ouyang B, Zhang Y, Li H, Ye Z (2016) Overexpression of calmodulin-like (ShCML44) stress-responsive gene from *Solanum habrochaites* enhances tolerance to multiple abiotic stresses. Sci Rep **6**: 31772

Pandey GK, Kanwar P, Singh A, Steinhorst L, Pandey A, Yadav AK, Tokas I, Sanyal SK, Kim BG, et al. (2015) Calcineurin B-Like protein-interacting protein kinase CIPK21 regulates osmotic and salt stress responses in *Arabidopsis*. Plant Physiol **169**: 780–792

Reddy ASN, Ali GS, Celesnik H, Day IS (2011) Coping with stresses: roles of calcium- and calcium/calmodulin-regulated gene expression. Plant Cell **23**: 2010–2032

Ronimus RS, Morgan HW (2003) Distribution and phylogenies of enzymes of the Embden-Meyerhof-Parnas pathway from archaea and hyperthermophilic bacteria support a gluconeogenic origin of metabolism. Archaea **1**: 199–221

Ruiz MCM, Hubbard KE, Gardner MJ, Jung HJ, Aubry S, Hotta CT, Mohd-Noh NI, Robertson FC, Hearn TJ, et al. (2018) Circadian oscillations of cytosolic free calcium regulate the *Arabidopsis* circadian clock. Nat Plants **4**: 690–698

Scholz SS, Reichelt M, Vadassery J, Mithofer A (2015) Calmodulin-like protein CML37 is a positive regulator of ABA during drought stress in *Arabidopsis*. Plant Signal Behav **10**: e1011951

Seppanen MM, Alitalo V, Backstrom HK, Makiniemi K, Jokela V, Falghera-Winseman L, Khazaei H (2018) Growth, freezing tolerance, and yield performance of alfalfa (*Medicago sativa* L.) cultivars grown under controlled and field conditions in northern latitudes. Can J Plant Sci **98**: 1109–1118

Sun Q, Huang R, Zhu H, Sun Y, Guo Z (2021) A novel *Medicago truncatula* calmodulin-like protein (MtCML42) regulates cold tolerance and flowering time. Plant J **108**: 1069–1082

Sun Q, Yu S, Guo Z (2020) Calmodulin-Like (CML) gene family in *Medicago truncatula*: genome-wide identification, characterization and expression analysis. Inter J Mol Sci **21**: 7142

Suzuki N, Koussevitzky S, Mittler R, Miller G (2012) ROS and redox signalling in the response of plants to abiotic stress. Plant Cell Environ **35**: 259–270

Tadege M, Wen JQ, He J, Tu HD, Kwak Y, Eschstruth A, Cayrel A, Endre G, Zhao PX, Chabaud M, et al. (2008) Large-scale insertional mutagenesis using the Tnt1 retrotransposon in the model legume *Medicago truncatula*. Plant J **54**: 335–347

Tan J, Wang C, Xiang B, Han R, Guo Z (2013) Hydrogen peroxide and nitric oxide mediated cold- and dehydration-induced myo-inositol phosphate synthase that confers multiple resistances to abiotic stresses. Plant Cell Environ **36**: 288–299

Vadassery J, Reichelt M, Hause B, Gershenzon J, Boland W, Mithofer A (2012) CML42-mediated calcium signaling coordinates responses to spodoptera herbivory and abiotic stresses in *Arabidopsis*. Plant Physiol **159**: 1159–1175

Wang Q, Shi H, Huang R, Ye R, Luo Y, Guo Z, Lu S (2021) AIR12 confers cold tolerance through regulation of the CBF cold response pathway and ascorbate homeostasis. Plant Cell Environ **44**: 1522–1533

Wang SS, Diao WZ, Yang X, Qiao Z, Wang M, Acharya BR, Zhang W (2015) *Arabidopsis thaliana* CML25 mediates the Ca^{2+} regulation of K^+ transmembrane trafficking during pollen germination and tube elongation. Plant Cell Environ **38**: 2372–2386

Wu X, Qiao Z, Liu H, Acharya BR, Li C, Zhang W (2017) CML20, an *Arabidopsis* calmodulin-like protein, negatively regulates guard cell ABA signaling and drought stress tolerance. Front Plant Sci **8**: 824

Xu B, Cheval C, Laohavisit A, Hocking B, Chiasson D, Olsson TSG, Shirasu K, Faulkner C, Gilliham M (2017) A calmodulin-like protein regulates plasmodesmal closure during bacterial immune responses. New Phytol **215**: 77–84

Xu J, Tian YS, Xing XJ, Peng RH, Zhu B, Gao JJ, Yao QH (2016) Over-expression of AtGSTU19 provides tolerance to salt, drought and methyl viologen stresses in *Arabidopsis*. Physiol Plant **156**: 164–175

Yang X, Wang SS, Wang M, Qiao Z, Bao CC, Zhang W (2014) *Arabidopsis thaliana* calmodulin-like protein CML24 regulates pollen tube growth by modulating the actin cytoskeleton and controlling the cytosolic Ca^{2+} concentration. Plant Mol Biol **86**: 225–236

Zhang LL, Zhao MG, Tian QY, Zhang WH (2011) Comparative studies on tolerance of *Medicago truncatula* and *Medicago falcata* to freezing. Planta **234**: 445–457

Zhang XX, Wang TZ, Liu M, Sun W, Zhang WH (2019) Calmodulin-like gene MtCML40 is involved in salt tolerance by regulating MtHKTs transporters in *Medicago truncatula*. Environ Exp Bot **157**: 79–90

Zhang Y, Ming R, Khan M, Wang Y, Dahro B, Xiao W, Li C, Liu J-H (2022) ERF9 of *Poncirus trifoliata* (L.) Raf. undergoes feedback regulation by ethylene and modulates cold tolerance via regulating a glutathione S-transferase U17 gene. Plant Biotechn J **20**: 183–200

Zhang ZQ, Hu XN, Zhang YQ, Miao ZY, Xie C, Meng XZ, Deng J, Wen JQ, Mysore KS, Frugie F, et al. (2016) Opposing control by transcription factors MYB61 and MYB3 increases freezing tolerance by relieving C-repeat binding factor suppression. Plant Physiol **172**: 1306–1323

Zhu JK (2016) Abiotic stress signaling and responses in plants. Cell **167**: 313–324

Zhu XY, Robe E, Jomat L, Aldon D, Mazars C, Galaud JP (2017) CML8, an *Arabidopsis* calmodulin-like protein, plays a role in *Pseudomonas syringae* plant immunity. Plant Cell Physiol **58**: 307–319

Zhu X, Wang P, Bai Z, Herde M, Ma Y, Li N, Liu S, Huang CF, Cui R, Ma H, et al. (2022) Calmodulin-like protein CML24 interacts with CAMTA2 and WRKY46 to regulate ALMT1-dependent Al resistance in *Arabidopsis thaliana*. New Phytol **233**: 2471–2487

Zhuo C, Liang L, Zhao Y, Guo Z, Lu S (2018) A cold responsive ethylene responsive factor from *Medicago falcata* confers cold tolerance by up-regulation of polyamine turnover, antioxidant protection, and proline accumulation. Plant Cell Environ **41**: 2021–2032

Zhuo C, Wang T, Lu S, Zhao Y, Li X, Guo Z (2013) A cold responsive galactinol synthase gene from *Medicago falcata* (*MfGolS1*) is induced by myo-inositol and confers multiple tolerances to abiotic stresses. Physiol Plant **149**: 67–78